A Strategic Finite Element Approach for Verification and Simulation of an Epidemiological Model for Dengue

Amanda Cabral, Edivaldo Junior

https://doi.org/10.1590/SciELOPreprints.12862

Submitted on: 2025-08-01
Posted on: 2025-08-04 (version 1)
(YYYY-MM-DD)

A STRATEGIC FINITE ELEMENT APPROACH FOR VERIFICATION AND SIMULATION OF AN EPIDEMIOLOGICAL MODEL FOR DENGUE

Amanda Maria Cardoso Cabral[1*] and Edivaldo Figueiredo Fontes Junior[2]

*Corresponding author
[1]Universidade Federal Rural do Rio de Janeiro, Seropédica, RJ, Brasil / ammcabrald@gmail.com / https://orcid.org/0009-0009-5393-0483
[2]Universidade Federal Rural do Rio de Janeiro, Seropédica, RJ, Brasil / edivaldofontes@gmail.com / https://orcid.org/0000-0001-7555-345X

ABSTRACT. This research describes a fundamental step in the study of the vital dynamics of dengue in the municipality of Seropédica, Rio de Janeiro: the development and validation of the Finite Element Method (FEM), combined with the Crank-Nicolson method and the Newton method. The simulation is described by the MSIR (Mosquito-Susceptible-Infected-Recovered) model, characterized by a system of nonlinear partial differential equations. The implementation and verification of the problem consisted of constructing a test problem with a known analytical solution. It was successfully verified, demonstrating that the maximum absolute error gradually decreases with the refinement of the spatial mesh, reaching an order of 10^{-4}. This work presents the activities funded by the Rio de Janeiro State Research Support Foundation (FAPERJ), developed at the Federal Rural University of Rio de Janeiro (UFRRJ).

Keywords: epidemiological model, dengue, finite element method.

1 Introduction

Dengue, transmitted by the *Aedes aegypti* mosquito, is one of the main diseases affecting Brazil and is a serious public health problem (Mendonça et al., 2009). There are four types of dengue virus (DENV-1, DENV-2, DENV-3, and DENV-4). Most individuals infected with the DENV-1 serotype have mild symptoms. Serotypes DENV-2, DENV-3, and DENV-4 cause symptoms such as high fever, body aches, pain behind the eyes, red spots, and nausea, which can progress to hemorrhagic dengue, which can have more serious consequences, such as bleeding, low blood pressure, dehydration, and risk of death, according to Barelli et al. (2023).

According to the Ministério da Saúde (2024), the first of this disease epidemic in Brazil occurred from 1981 to 1982 in Boa Vista (RR), caused by serotypes 1 and 4. Four years later, in 1986, epidemics occurred in the state of Rio de Janeiro and some capitals in the Northeast region. In some parts of the country, the climate is hotter and more humid, favoring the proliferation of mosquitoes and the spread of the disease.

Global climate change is a key factor in this growth. With global warming, there are longer periods of heat, which have an impact on the increase in the number of cases. In the last 25 years, around 18 million Brazilians have been infected with the virus, and the highest number of cases in Brazil's history is projected to be reached in 2024, according to Gurgel-Gonçalves et al. (2024).

In addition to factors such as the hot and humid environment, the accumulation of water in containers, vases, and tires due to heavy rains contributes to the formation of mosquito larvae. Furthermore, the movement of infected people in these areas favors the spread of dengue, since the mosquito can bite a person infected with the *Aedes aegypti* virus and transmit it to another susceptible person, thus forming a cycle and generating a new epidemic.

Located in the state of Rio de Janeiro, the municipality of Seropédica, according to data from Instituto Brasileiro de Geografia e Estatística (IBGE) (2024), had approximately 80,596 inhabitants and a land area of 265,189 km^2 in 2022, with a population density of 303.92 km^2. The estimated population in 2024 was 84,737 people, also according to Instituto Brasileiro de Geografia e Estatística (IBGE) (2024).

There are a total of 18 neighborhoods in the municipality, namely: Boa Esperança, Cabral, Campo Lindo, Canto do Rio neighborhood, Carretão neighborhood, Chaperó neighborhood, Ecologia neighborhood, Fazenda Caxias neighborhood, Incra neighborhood, Jardim Maracanã neighborhood, Jardins neighborhood, Nazaré neighborhood, Parque Jacimar neighborhood, Piranema neighborhood, Santa Alice neighborhood, Santa Sofia neighborhood, São Miguel neighborhood, and UFRRJ neighborhood. The neighborhoods of Seropédica were obtained from MBI Brasil (2024), and are represented in the Seropédica regions below, as shown in the Figure 1.

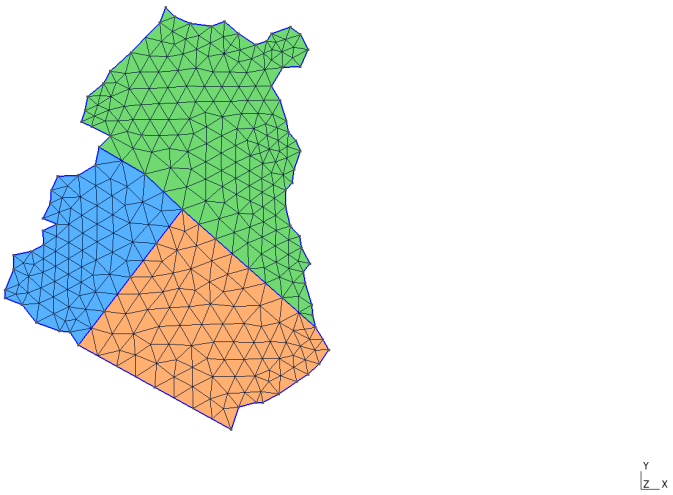

Figure 1: Domain divided into three distinct regions.

Where, in each region, the neighborhoods are located:

- **Region 1 (Blue)**: Covers the neighborhoods of Piranema, UFRRJ, Parque Jacimar, Campo Lindo, and Canto do Rio.
- **Region 2 (Orange)**: This region is formed by the neighborhoods of Chaperó, Santa Sofia, and Fazenda Caxias.
- **Region 3 (Green)**: Characterized by the neighborhoods of Boa Esperança, Ecologia, Incra, Jardins, Jardim Maracanã, Santa Alice, São Miguel, Carretão, Cabral, and Nazaré.

In a data survey, it was observed that some research conducted by the Prefeitura Municipal de Seropédica (2023), in Rio de Janeiro, indicated that in December 2023, the incidence of this disease was high. Added to this, the vectors scattered throughout the municipality, the turnover of residents, the likely locations with standing water, and the summer season favor an increase in cases over the coming months. This raises the question: Can modeling the dynamics of the disease in the area predict and prevent future epidemics?

In this study, we applied a derivation of the SIR model and performed a validation and verification of the model to understand how dengue behaves under the socio-environmental factors mentioned above, as well as to observe focal points of incidence over the months in Seropédica, Rio de Janeiro.

The validation of the SIR model and its variants can show how computational modeling, in the epidemiological context, applied to analyze and simulate the behavior of diseases,

is a valuable tool. In particular, its variant, known as the MSIR (Susceptible-Infected-Recovered) epidemiological model. After validating the model, it will be possible to simulate the behavior of dengue in the municipality of Seropédica, Rio de Janeiro, throughout the summer season, which has high rainfall rates and a considerable number of reported cases of disease. In addition to visualizing where cases are most concentrated, there will be more opportunities for control and intervention.

With the benefits of simulating the evolutionary behavior of the disease, SIR modeling and its variations can be used to control and intervene in the spread of numerous diseases.

2 Epidemiological Modeling and Test Problem with Exact Solution

2.1 The Classic SIR Epidemiological Model

To investigate the progression of this disease, a variant of the classic SIR epidemiological model was used, characterized by the compartments: susceptible S, infected I, and recovered R. In this study, these categories represent the total population residing in Seropédica.

The SIR model (1)-(3) was developed in 1927 by mathematicians and epidemiologists William Ogilvy Kermack and Anderson Gray McKendrick and proposed in the article "A Contribution to the Mathematical Theory of Epidemics" (Kermack and McKendrick, 1927). This work describes how a disease spreads over time using a system of differential equations. For the mathematical formulation of the problem, the work of Gomes (2009) was adopted, resulting in the following system of equations:

$$\frac{\partial \mathbf{S}}{\partial t} = -\beta \mathbf{SI}; \tag{1}$$

$$\frac{\partial \mathbf{I}}{\partial t} = \beta \mathbf{SI} - \sigma \mathbf{I}; \tag{2}$$

$$\frac{\partial \mathbf{R}}{\partial t} = \sigma \mathbf{I}; \tag{3}$$

They represent:

$\frac{\partial \mathbf{S}}{\partial t}$**:** Represents the dynamics of susceptible individuals over time.

$\frac{\partial \mathbf{I}}{\partial t}$**:** Represents the dynamics of infected individuals over time.

$\frac{\partial \mathbf{R}}{\partial t}$**:** Represents the dynamics of recovered individuals over time.

The compartments, coefficients, and parameters are:

- **S**: Susceptible population (not yet infected).

- **I**: Infected population (capable of transmitting the disease).
- **R**: Recovered population (immune to the disease).
- β: Parameter indicating the speed of disease transmission.
- σ: Parameter indicating the speed of recovery from the disease.

According to Almeida (2014), the compartmental scheme of the SIR model, adapted in this work, can be illustrated in Figure 2:

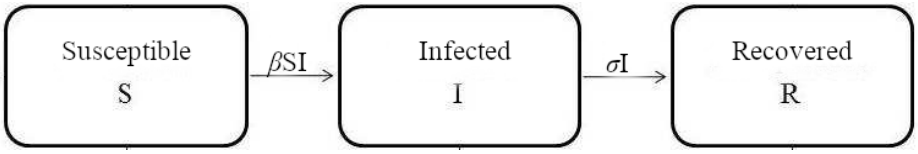

Figure 2: Compartmental diagram of the SIR model.

Each differential equation of the SIR (susceptible-infected-recovered) model describes the dynamics of the compartments S, I, R at each time step t_s of the simulation in a location. The negative sign in equation (1) indicates that the number of individuals susceptible to the disease decreases over time, as they become infected individuals.

In addition, the SIR model is guided by concepts, one of the main ones being William Hammer's Principle of Mass Action (1906) (Hamer, 1906), which brought the Guldberg-Waage Law (Atkins and de Paula, 2018) to epidemiology. Hammer's Principle of Mass Action states that the number of susceptible individuals and the number of infected individuals is directly proportional to the infection rate βSI, and the recovery rate σI is proportional to the number of infected individuals.

It should be added that additional conditions were used to model the progression of dengue disease in this initial stage, such as permanent immunization of infected individuals after their recovery. The group of individuals who moved from the infected compartment I to the recovered compartment R will not become susceptible S again. This condition would only be different if the model used were a variant of the SIR model, such as the SIRS model (susceptible-infected-recovered-susceptible).

The total population of infected, susceptible, and recovered individuals is considered constant N at the location, where $N = S + I + R$ throughout the simulation period, assuming that there is no inflow or outflow of people from the location where the spread of the disease is simulated and that the birth and death rates are zero.

In addition, the total population is considered homogeneous, that is, it is well distributed in the simulation location and all individuals have the same chance of being infected by the disease. There are no locations where a greater or lesser number of individuals reside. The model also considers that as soon as an individual is infected, they will become highly infectious; there is no specific time until the person becomes infectious.

The SIR model (1)-(3) assumes that the parameters σ (parameter indicating the speed of recovery from the disease) and β (parameter indicating the speed of infection) will

remain constant over the simulation time t_s. In future simulations, a variant will be used in which there are variations over time, collecting more data and socio-environmental factors for the study of dengue transmission.

2.2 The MSIR Epidemiological Model

As the research was based on disease progression, a variant of the SIR model was used. For this reason, the SIR model was expanded from three compartments (S, I, R) to four compartments (M, S, I, R), in which the compartment of mosquitoes that transmit was included.

The MSIR model studied was adapted from the master's thesis by Luciana Takata Gomes, who states that the vital dynamics of the mosquito are Malthusian (the rate of population change is proportional to the quantity) (Gomes, 2009). In addition, Gomes (2009)'s work proposes that this model is considered simple and well suited for a short period of time and conditions favorable to reproduction.

The MSIR model consisted of four partial differential equations and the domain Ω, shown in Figure 3, in which the model was simulated is the region of the municipality of Seropédica itself. The time evaluated for simulation was during the period from December 2023 to February 2024.

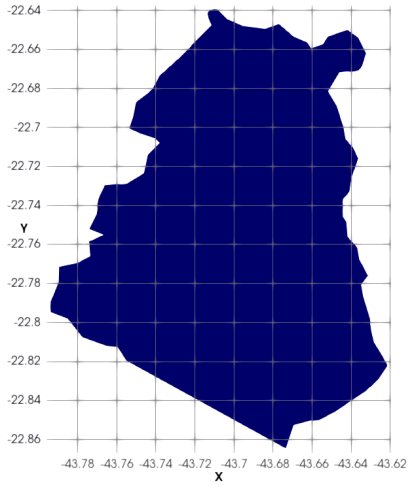

Figure 3: Spatial domain Ω of the model.

The state variables M, S, I, R of the model are functions that depend on time and geographical position (x, y) of the continuous spatial domain Ω of Seropédica. These variables describe the state of M, S, I, R at any time t chosen at a given position (x, y) in the spatial domain.

$$\mathbf{M} = M(x, y, t); \tag{4}$$
$$\mathbf{S} = S(x, y, t); \tag{5}$$
$$\mathbf{I} = I(x, y, t); \tag{6}$$
$$\mathbf{R} = R(x, y, t) \tag{7}$$

The MSIR model was characterized by the system of equations (8)-(11), adapted from Gomes (2009):

$$\frac{\partial \mathbf{M}}{\partial t} = f_0 + \nabla \cdot (\alpha_M \nabla \mathbf{M}) + \nu \mathbf{M} - \mu \mathbf{M} \tag{8}$$
$$\frac{\partial \mathbf{S}}{\partial t} = f_1 + \nabla \cdot (\alpha_H \nabla \mathbf{S}) - \beta \mathbf{M}\ \mathbf{S} \tag{9}$$
$$\frac{\partial \mathbf{I}}{\partial t} = f_2 + \nabla \cdot (\alpha_H \nabla \mathbf{I}) + \beta \mathbf{S}\mathbf{M} - \sigma \mathbf{I} \tag{10}$$
$$\frac{\partial \mathbf{R}}{\partial t} = f_3 + \nabla \cdot (\alpha_R \nabla \mathbf{R}) + \sigma \mathbf{I}; \tag{11}$$

which can be rewritten as:

$$\frac{\partial \mathbf{M}}{\partial t} - \nabla \cdot (\alpha_M \nabla \mathbf{M}) - \nu \mathbf{M} + \mu \mathbf{M}\ = f_0; \tag{12}$$
$$\frac{\partial \mathbf{S}}{\partial t} - \nabla \cdot (\alpha_H \nabla \mathbf{S}) + \beta \mathbf{M}\mathbf{S}\ = f_1; \tag{13}$$
$$\frac{\partial \mathbf{I}}{\partial t} - \nabla \cdot (\alpha_H \nabla \mathbf{I}) - \beta \mathbf{S}\mathbf{M} + \sigma I\ = f_2; \tag{14}$$
$$\frac{\partial \mathbf{R}}{\partial t} - \nabla \cdot (\alpha_R \nabla \mathbf{R}) - \sigma \mathbf{I} = f_3; \tag{15}$$

They represent:

$\frac{\partial \mathbf{M}}{\partial t}$**:** Represents the dynamics of vectors over time.

$\frac{\partial \mathbf{S}}{\partial t}$**:** Represents the dynamics of susceptible individuals over time.

$\frac{\partial \mathbf{I}}{\partial t}$**:** Represents the dynamics of infected individuals over time.

$\frac{\partial \mathbf{R}}{\partial t}$**:** Represents the dynamics of recovered individuals over time.

The compartments, coefficients, and parameters are:

- **M**: Transmitting mosquitoes.
- **S**: Susceptible population (not yet infected).

- **I**: Infected population (capable of transmitting the disease).
- **R**: Recovered population (immune to the disease).
- β: Parameter indicating the speed of disease transmission.
- σ: Parameter indicating the speed of recovery from the disease.
- ν: Parameter indicating the birth rate of the mosquito.
- μ: Parameter indicating the mortality rate of the mosquito.
- $\alpha_{\mathbf{M}}$: Coefficient indicating the dispersion of mosquitoes.
- $\alpha_{\mathbf{H}}$: Coefficient indicating the dispersion of susceptible individuals.
- $\alpha_{\mathbf{R}}$: Coefficient indicating the dispersion of mosquitoes.

The MSIR model, according to Gomes (2009) research, considers only one compartment for mosquitoes. Compartment M is considered an average of dengue vector mosquitoes. The MSIR model has six parameters, with β and σ coming from the SIR model and ν and μ, which represent the birth and death rates of mosquitoes. The coefficients $\alpha_{\mathbf{M}}$, $\alpha_{\mathbf{H}}$, and $\alpha_{\mathbf{R}}$ are accompanied by expressions such as $\nabla \cdot \alpha_{\mathbf{M}} \nabla \mathbf{M}$, $\nabla \cdot \alpha_{\mathbf{H}} \nabla \mathbf{S}$, and $\nabla \cdot \alpha_{\mathbf{H}} \nabla \mathbf{I}$. These expressions indicate how dispersed dengue-transmitting mosquitoes and humans are throughout the region and also the flow out of areas of concentration. In this case, the municipality of Seropédica.

The terms f_0, f_1, f_2 and f_3 on the right side of system (12)-(15) are called source terms and indicate extra data, respectively, on how M, S, I, R vary over time t due to factors that can be complex to present in a parameter, such as precipitation, insecticide spraying, and accumulated containers. In this research, the source terms were defined by equations (16)-(19).

$$f_0 = 2\pi^2 e^{-t} \sin(\pi x) \sin(\pi y) - e^{-t} \sin(\pi x) \sin(\pi y); \tag{16}$$

$$f_1 = e^{-2t} \sin^2(\pi x) \cos(\pi x) \sin(\pi y) + 38.47841760435743 e^{-t} \sin(\pi x) \cos(\pi x); \tag{17}$$

$$f_2 = (t + x + y) - e^{-2t} \sin^2(\pi x) \cos(\pi x) \sin(\pi y) + 1; \tag{18}$$

$$f_3 = -(t + x + y) - 3e^{-t+x+y}.; \tag{19}$$

The source terms f_0, f_1, f_2 and f_3 are functions of the spatial coordinates (x, y) of the domain Ω for a certain instant of time t. The term f_0 indicates an exponential reduction in mosquitoes over time influenced by external factors. In f_1 and f_3, their components also indicate an exponential reduction over time. However, the term f_2 shows temporal growth.

The choice of specific functions for the components f_0, f_1, f_2 and f_3 does not aim, for now, to simulate a realistic model, but rather to validate a test problem to verify the computational code and methods that will be used to solve it.

The MSIR model presents an evolutionary dynamic that can be represented by the compartmental scheme in Figure 4, extracted from Gomes (2009), in which all susceptible individuals will be infected and subsequently recover during the simulation.

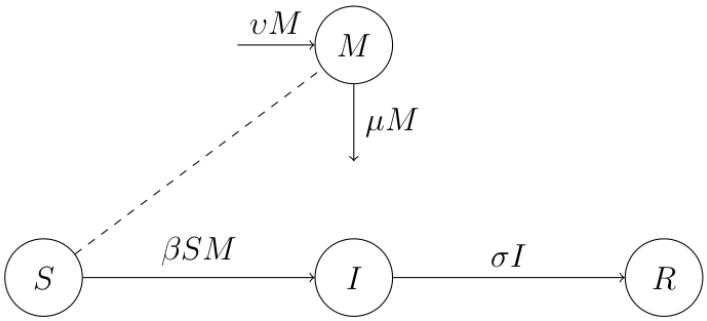

Figure 4: Compartmental diagram of the MSIR model.

Therefore, before applying the epidemiological model to a realistic scenario, it is a necessary methodological step to construct a test problem to verify the accuracy of the numerical tool. The next step in this work is to present in detail the process of constructing and validating the computational solver.

3 Procedures and Methodology

In this study, we used a modified SIR model consisting of four EDPs (12)-(15) that describe the evolution of dengue by compartments, such as mosquito vectors M, individuals susceptible to the disease S, infected I, and recovered R

The variables M, S, I, and R are the state variables of the problem, Ω is the domain represented by the Seropédica map, t_s is the simulation time, and f_0, f_1, f_2, and f_3 are the source terms. The states variable M, S, I, R are fundamental to the configuration of the MSIR model. They are the independent variables of the system and describe the state of each compartment at a given moment in time.

To validate the computational implementation, a test problem was constructed from the nonlinear system of PDEs (8)-(11), defining the following exact solution for this problem:

$$\mathbf{M}(x, y, t) = e^{-t} \sin(\pi x) \sin(\pi y); \tag{20}$$

$$\mathbf{S}(x, y, t) = e^{-t} \sin(\pi x) \cos(\pi x); \tag{21}$$

$$\mathbf{I}(x, y, t) = x + y + t; \tag{22}$$

$$\mathbf{R}(x, y, t) = e^{x+y-t}. \tag{23}$$

Through algebraic manipulations and knowing the source terms (16)-(19), other components of the nonlinear system of PDEs (12)-(15) were found, such as the initial conditions

and boundary conditions. The solver used is based on that used in the authors' references Santos et al. (2022) and do Carmo et al. (2024).

The initial conditions (24)-(27) are the solutions of M, S, I, R of the problem at the initial time $t = 0$ throughout the municipality of Seropédica:

$$\mathbf{M}(x, y, 0) = \sin(\pi x)\sin(\pi y); \tag{24}$$

$$\mathbf{S}(x, y, 0) = \sin(\pi x)\cos(\pi x); \tag{25}$$

$$\mathbf{I}(x, y, 0) = x + y; \tag{26}$$

$$\mathbf{R}(x, y, 0) = e^{x+y}. \tag{27}$$

The boundary conditions are the solutions M, S, I, R of the problem across the entire boundary of the municipality of Seropédica and are prescribed according to the exact solution (20)-(23).

Since this is a validation of a test problem for the MSIR model, the parameters ν (indicates the mosquito birth rate), μ (indicates the mosquito mortality rate), σ (indicates the disease recovery rate), β (indicates the disease transmission rate), and coefficients α_M (indicates mosquito dispersion), α_H (indicates individual dispersion), α_R (indicates recovered individual dispersion) of the ODE system were considered equal to 1 (dimensionless) and the simulation time ranging from 0 to 1 (dimensionless).

The selection of dimensionless parameters is based on the test problem and verification of the computational implementation, ensuring accuracy regardless of the complexity of the real data or units. In future simulations, these parameters will be modified based on realistic and geographic data.

The validation process of the PDEs system implemented for the MSIR model consisted of searching for an approximate solution for M, S, I, R, in relation to the pre-established exact solution. The methods used to solve the nonlinear system of PDEs were: Finite Element Method, Crank-Nicolson method, and Newton's method.

If the solver finds an approximate solution for M, S, I, R with the smallest possible error, a computer simulation of the evolutionary behavior of dengue will be initiated, with greater precision in the parameters, coefficients, and data from Seropédica. The errors were defined from equations in which, for each state of variable, the exact solution of the problem, given by (20)-(23), is subtracted from the approximate solution by the FEM obtained by the authors.

3.1 Finite Element Method

In biological phenomena, analytical solutions are almost impossible to find. Therefore, we use the numerical tool to solve the test problem (8)-(11), known as the Finite Element Method (FEM) (Hughes and Hughes, 2000). The FEM is a technique widely used in solving problems related to applications in heat transfer, elasticity, fluid mechanics, and dynamic behavior of structures, and seeks an approximate solution with the smallest possible residue for the problem.

The implementation of the Finite Element Method solves the problem by discretizing the spatial domain Ω, that is, by forming regular geometric divisions of the domain (mesh). With the help of the Gmsh *software* (Geuzaine and Remacle, 2009), a mesh representing the municipality of Seropédica was generated. In this mesh, the geometric divisions are called finite elements and were represented by triangles. All finite elements are connected by nodal points or finite element nodes (vertices of the triangles). The triangular element was chosen because it is the geometric figure that best adapts to the contours of complex domains, such as the map of the municipality of Seropédica.

The more refined the mesh, the closer the approximate solution to the problem will be to the actual solution, resulting in increasingly smaller residuals. For this, the nodes and geometric elements must be sufficiently refined by the spatial domain Ω of the model and have a small area.

In the Finite Element Method, each element has a basis function associated with each of its nodes. Basis functions (28) are used to approximate the solution in each finite element, interpolating the variables M, S, I, R to the vertices of the elements. The basis function ϕ is a linear function and varies linearly between 0 and 1. That is, if V_i is a vertex of the triangle for $i = 1, 2, 3$, then:

$$\phi_j(V_i) = \begin{cases} 1 & \text{se } i = j \\ 0, & \text{se } i \neq j \end{cases} \tag{28}$$

The approximate solution $\mathbf{u}(x, y)$ (29) inside a triangular element is a linear combination of the basis functions, where u_1, u_2, and u_3 are the values of the solution at each node:

$$\mathbf{u}(x, y) = u_1 \cdot \phi_1(x, y) + u_2 \cdot \phi_2(x, y) + u_3 \cdot \phi_3(x, y) \tag{29}$$

For a set of triangles, i.e., a mesh, the global approximate solution $\mathbf{U}(x, y)$ is given as the sum of the approximate solutions in each triangular element. Since this is a simulation of the vital dynamics of dengue, the simulation time, denoted by t, must be included. Thus, the global solution (30) can be represented by:

$$\mathbf{U}(x, y, t) = \sum_{j=1}^{n_{\text{vértices}}} u_j \cdot \phi_j(x, y) \tag{30}$$

- Galerkin method

The Galerkin method creates a system for partial differential equations with the aim of finding the values of the quantities M_j, S_j, I_j, R_j for $j = 1, 2, 3$, which are the approximate solutions at each node of the triangular element.

From (30), the approximate global solutions for each quantity M, S, I, R can be described as in equations (31)-(34):

$$\mathbf{M}_g(x,y,t) = \sum_{j=1}^{n_{\text{vértices}}} m_j \cdot \phi_j(x,y); \tag{31}$$

$$\mathbf{S}_g(x,y,t) = \sum_{j=1}^{n_{\text{vértices}}} s_j \cdot \phi_j(x,y); \tag{32}$$

$$\mathbf{I}_g(x,y,t) = \sum_{j=1}^{n_{\text{vértices}}} i_j \cdot \phi_j(x,y); \tag{33}$$

$$\mathbf{R}_g(x,y,t) = \sum_{j=1}^{n_{\text{vértices}}} r_j \cdot \phi_j(x,y); \tag{34}$$

In each three-node element, for each quantity M, S, I, R, the local solutions can be described as in equations (35)-(38):

$$\mathbf{M}_e(x,y,t) = m_1(t)\cdot\phi_1(x,y) + m_2(t)\cdot\phi_2(x,y) + m_3(t)\cdot\phi_3(x,y); \tag{35}$$

$$\mathbf{S}_e(x,y,t) = s_1(t)\cdot\phi_1(x,y) + s_2(t)\cdot\phi_2(x,y) + s_3(t)\cdot\phi_3(x,y); \tag{36}$$

$$\mathbf{I}_e(x,y,t) = i_1(t)\cdot\phi_1(x,y) + i_2(t)\cdot\phi_2(x,y) + i_3(t)\cdot\phi_3(x,y); \tag{37}$$

$$\mathbf{R}_e(x,y,t) = r_1(t)\cdot\phi_1(x,y) + r_2(t)\cdot\phi_2(x,y) + r_3(t)\cdot\phi_3(x,y); \tag{38}$$

The nonlinear differential equations of the MSIR model describe the behavior of each compartment, representing all temporal and spatial iterations. Since we seek an exact solution, there will be a residue at least at one point in the spatial domain Ω. Therefore, the global solution does not satisfy the corresponding partial differential equation. The residue can be expressed by the equations (39)-(42):

$$R_M = \frac{\partial \mathbf{M}_g}{\partial t} - \nabla\cdot(\alpha_M \nabla \mathbf{M}_g) - \nu\mathbf{M}_g + \mu\mathbf{M}_g - f_0; \tag{39}$$

$$R_S = \frac{\partial \mathbf{S}_g}{\partial t} - \nabla\cdot(\alpha_H \nabla \mathbf{S}_g) + \beta\mathbf{M}_g\mathbf{S}_g - f_1; \tag{40}$$

$$R_I = \frac{\partial \mathbf{I}_g}{\partial t} - \nabla\cdot(\alpha_H \nabla \mathbf{I}_g) - \beta\mathbf{S}_g\mathbf{M}_g + \sigma\mathbf{I}_g - f_2; \tag{41}$$

$$R_R = \frac{\partial \mathbf{R}_g}{\partial t} - \nabla\cdot(\alpha_R \nabla \mathbf{R}_g) - \sigma\mathbf{I}_g - f_3. \tag{42}$$

The Galerkin method reduces the residual through the inner product with a test function $\mathbf{v}_n$, seeking to make the residual orthogonal to the test function v_n (equivalent to the basis function ϕ_j), where n is the number of vertices, expressed in the equation (43) below:

$$< R_{\text{EDP}}, \mathbf{v}_n >= \int_\Omega R_{\text{EDP}} \cdot \mathbf{v}_n \, d\Omega = 0 \tag{43}$$

Through algebraic manipulations, for M, we find (44)-(45):

$$\int_{\Omega}\left[\frac{\partial \mathbf{M}_g}{\partial t}-\nabla\cdot(\alpha_M\nabla\mathbf{M}_g)-\nu\mathbf{M}_g+\mu\mathbf{M}_g-f_0\right]\cdot\mathbf{v}_n\,d\Omega=0; \tag{44}$$

$$\int_{\Omega}\frac{\partial \mathbf{M}_g}{\partial t}\cdot\mathbf{v}_n d\Omega-\int_{\Omega}\left[\nabla\cdot(\alpha_M\nabla\mathbf{M}_g\right]\cdot\mathbf{v}_n d\Omega-\int_{\Omega}(\nu\mathbf{M}_g-\mu\mathbf{M}_g+f_0)\cdot\mathbf{v}_n d\Omega=0; \tag{45}$$

Using the Divergence Theorem in this component (46):

$$-\int_{\Omega}\left[\nabla\cdot(\alpha_M\nabla\mathbf{M}_g)\right]\cdot\mathbf{v}_n\,d\Omega \tag{46}$$

We obtain (47):

$$-\int_{\Omega}\left[\nabla\cdot(\alpha_M\nabla\mathbf{M}_g)\right]\cdot\mathbf{v}_n\,d\Omega=+\int_{\Omega}(\alpha_M\nabla\mathbf{M}_g)\cdot(\nabla\mathbf{v}_n)\,d\Omega-\int_{\partial\Omega}(\alpha_M\nabla\mathbf{M}_g\cdot\mathbf{n})\mathbf{v}_n\,dS \tag{47}$$

Finally, it results in (48):

$$\int_{\Omega}\frac{\partial \mathbf{M}_g}{\partial t}\cdot\mathbf{v}_n d\Omega+\int_{\Omega}(\alpha_M\nabla\mathbf{M}_g)\cdot(\nabla\mathbf{v}_n)d\Omega-\int_{\Omega}(\nu\mathbf{M}_g-\mu\mathbf{M}_g+f_0)\mathbf{v}_n d\Omega=$$
$$\int_{\partial\Omega}(\alpha_M\nabla\mathbf{M}_g\cdot\mathbf{n})\mathbf{v}_n dS \tag{48}$$

For the partial differential equation of the susceptible compartment S, remembering that the residue is of the form (49):

$$R_S=\frac{\partial \mathbf{S}_g}{\partial t}-\nabla\cdot(\alpha_H\nabla\mathbf{S}_g)+\beta\mathbf{M}_g\mathbf{S}_g-f_1; \tag{49}$$

We can obtain (50)-(51) through the vector product:

$$\int_{\Omega}\left[\frac{\partial \mathbf{S}_g}{\partial t}-\nabla\cdot(\alpha_H\nabla\mathbf{S}_g)+\beta\mathbf{M}_g\mathbf{S}_g-f_1\right]\cdot\mathbf{v}_n\,d\Omega=0; \tag{50}$$

$$\int_{\Omega}\frac{\partial \mathbf{S}_g}{\partial t}\cdot\mathbf{v}_n d\Omega-\int_{\Omega}\left[\nabla\cdot(\alpha_H\nabla\mathbf{S}_g)\right]\cdot\mathbf{v}_n d\Omega+\int_{\Omega}(\beta\mathbf{M}_g\mathbf{S}_g-f_1)\cdot\mathbf{v}_n d\Omega=0; \tag{51}$$

The weak form for EDP related to susceptible individuals S, by the Divergence Theorem, will be of the form (52):

$$\int_\Omega \frac{\partial \mathbf{S}_g}{\partial t} \cdot \mathbf{v}_n d\Omega + \int_\Omega (\alpha_H \nabla \mathbf{S}_g) \cdot (\nabla \mathbf{v}_n) d\Omega + \int_\Omega \beta \mathbf{M}_g \mathbf{S}_g \cdot \mathbf{v}_n d\Omega - \int_\Omega f_1 \cdot \mathbf{v}_n d\Omega = \int_{\partial\Omega} (\alpha_H \nabla \mathbf{S}_g \cdot \mathbf{n}) \mathbf{v}_n dS \quad (52)$$

For the differential equation linked to infected individuals I, the corresponding residual has the equation (53):

$$R_I = \frac{\partial \mathbf{I}_g}{\partial t} - \nabla \cdot (\alpha_H \nabla \mathbf{I}_g) - \beta \mathbf{S}_g \mathbf{M}_g + \sigma \mathbf{I}_g - f_2; \quad (53)$$

The vector product results in the equations (54)-(55):

$$\int_\Omega \left[\frac{\partial \mathbf{I}_g}{\partial t} - \nabla \cdot (\alpha_H \nabla \mathbf{I}_g) - \beta \mathbf{S}_g \mathbf{M}_g + \sigma \mathbf{I}_g - f_2 \right] \cdot \mathbf{v}_n \, d\Omega = 0 \quad (54)$$

$$\int_\Omega \frac{\partial \mathbf{I}_g}{\partial t} \cdot \mathbf{v}_n d\Omega - \int_\Omega [\nabla \cdot (\alpha_H \nabla \mathbf{I}_g)] \cdot \mathbf{v}_n d\Omega - \int_\Omega (\beta \mathbf{S}_g \mathbf{M}_g - \sigma \mathbf{I}_g + f_2) \cdot \mathbf{v}_n d\Omega = 0; \quad (55)$$

Similarly, we obtain the equation (56):

$$\int_\Omega \frac{\partial \mathbf{I}_g}{\partial t} \cdot \mathbf{v}_n d\Omega + \int_\Omega (\alpha_H \nabla \mathbf{I}_g) \cdot (\nabla \mathbf{v}_n) d\Omega - \int_\Omega (\beta \mathbf{M}_g \mathbf{S}_g - \sigma \mathbf{I}_g) \cdot \mathbf{v}_n d\Omega - \int_\Omega f_2 \cdot \mathbf{v}_n d\Omega = \int_{\partial\Omega} (\alpha_H \nabla \mathbf{I}_g \cdot \mathbf{n}) \mathbf{v}_n dS \quad (56)$$

Regarding the partial differential equation of recovered individuals M, the following equations (57)-(58) result directly from the vector product:

$$\int_\Omega \left[\frac{\partial \mathbf{R}_g}{\partial t} - \nabla \cdot (\alpha_R \nabla \mathbf{R}_g) - \sigma \mathbf{I}_g - f_3 \right] \cdot \mathbf{v}_n \, d\Omega = 0 \quad (57)$$

$$\int_\Omega \frac{\partial \mathbf{R}_g}{\partial t} \cdot \mathbf{v}_n d\Omega - \int_\Omega [\nabla \cdot (\alpha_R \nabla \mathbf{R}_g)] \cdot \mathbf{v}_n d\Omega - \int_\Omega (\sigma \mathbf{I}_g + f_3) \cdot \mathbf{v}_n d\Omega = 0; \quad (58)$$

By the Divergence Theorem, it implies that (59):

$$\int_\Omega \frac{\partial \mathbf{R}_g}{\partial t} \cdot \mathbf{v}_n d\Omega + \int_\Omega (\alpha_R \nabla \mathbf{R}_g) \cdot (\nabla \mathbf{v}_n) d\Omega - \int_\Omega (\sigma \mathbf{I}_g) \cdot \mathbf{v}_n d\Omega - \int_\Omega f_3 \cdot \mathbf{v}_n d\Omega = \int_{\partial\Omega} (\alpha_R \nabla \mathbf{R}_g \cdot \mathbf{n}) \mathbf{v}_n dS \quad (59)$$

These are the weak forms of the partial differential equations referring to the MSIR model. The weak form equations result in a large system of nonlinear differential equations, where we seek the values of m_j, s_j, i_j, r_j, corresponding to the values of the solutions at the nodes of the triangular elements. This system is sparse due to the definition of the basis function ϕ_j, which is nonzero only at the nodal points that have the same triangular element in common.

- Crank-Nicolson Method and Newton's Method

The Crank-Nicolson method (Crank and Nicolson, 1947) was used for temporal discretization and the Newton method (Burden and Faires, 2011) to receive the system of nonlinear PDEs and linearize it to solve iteratively at each time step. The discretization of the time line t_s, relative to the simulation time of the test problem, was 10 intervals.

$$[0 \xrightarrow{tol=10^{-8}} 0.1 \xrightarrow{tol=10^{-8}} 0.2 \xrightarrow{tol=10^{-8}} ... \xrightarrow{tol=10^{-8}} 1)$$

The stopping criterion considered for Newton's method at each time interval was 10^{-8}. That is, at each time step, Newton's method iterates until the solution reached is less than 10^{-8}.

4 Results obtained

The discretization of the continuous spatial domain Ω was performed using Gmsh *software*. The *software* can be used to generate a mesh from a file containing the latitude and longitude coordinates of the domain boundary. In total, the first mesh generated had 473 nodes and 860 triangular finite elements, as shown in Figure 5.

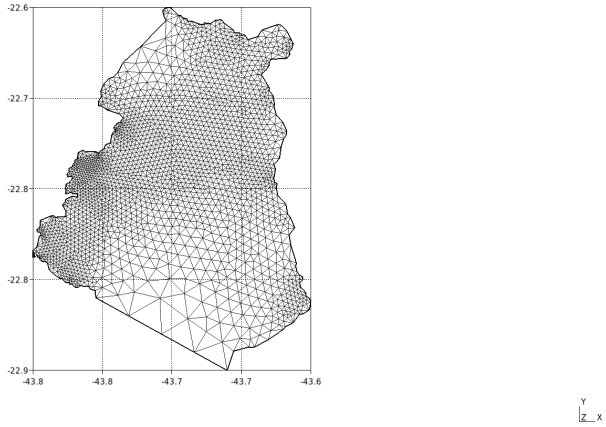

Figure 5: Initial discretization of the spatial domain Ω of the model.

The ParaView *software* Ahrens et al. (2005) was used, into which a file containing the mesh data generated by Gmsh was submitted. In ParaView, a proprietary calculator was used to return the residual of the solution found by the FEM. In these equations, for each state variable M, S, I, R, the previously defined exact solution of the problem was subtracted from the approximate solution by MEF. Thus, a graph was generated with a color scale ranging from 0 to the maximum absolute error. In red, it was indicated where the approximate solution obtained by FEM obtained the maximum absolute error. For each compartment, a graph with a color scale was generated:

- Error graph for the initial discretization of the spatial domain Ω:

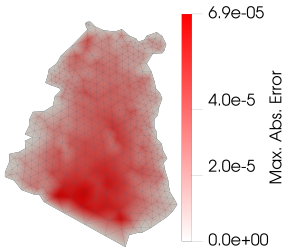

(a) Dengue vectors.

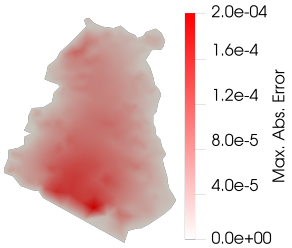

(b) Susceptible individuals.

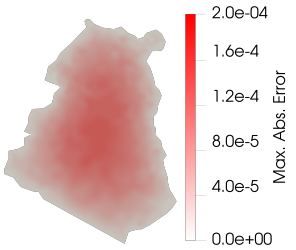

(c) Infected individuals.

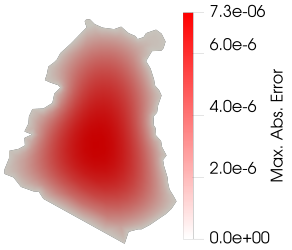

(d) Recovered individuals.

Figure 6: Maximum absolute error for each state variable.

For a better solution, a more refined mesh is needed. The initial mesh was not sufficiently refined and therefore obtained a still considerable maximum absolute error. The initial file submitted to the Gmsh *software* was manipulated, removing some points from its contour that were too close together. The removal of the points does not interfere with the method and made it possible to generate a more uniform mesh from the first one. The new discretization in the Figure 7 consisted of 893 nodal points and 1672 finite elements.

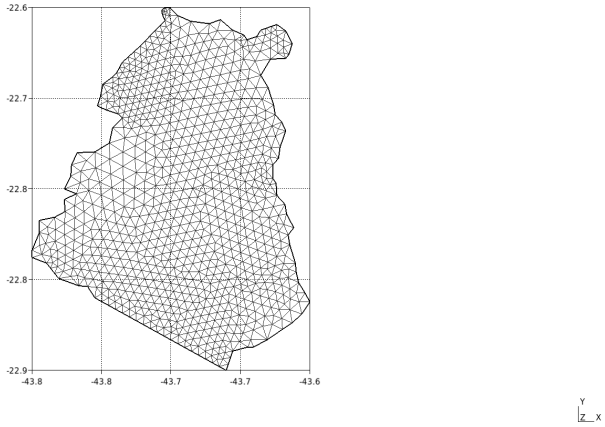

Figure 7: Second discretization of the spatial domain Ω of the model.

The process was redone to calculate the maximum absolute error for each compartment M, S, I, R in the ParaView *software*, and is shown in the graphs below:

- Error graph for the second discretization of the spatial domain Ω:

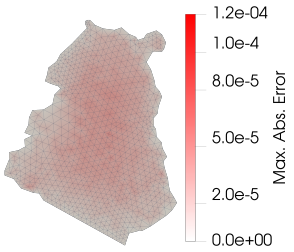

(a) Dengue vectors.

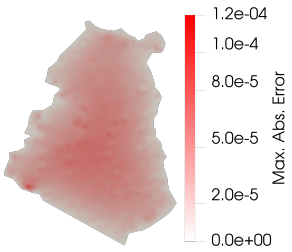

(b) Susceptible individuals.

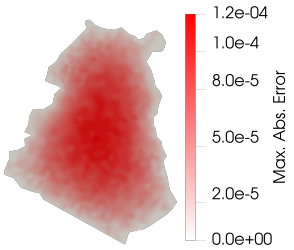

(c) Infected individuals.

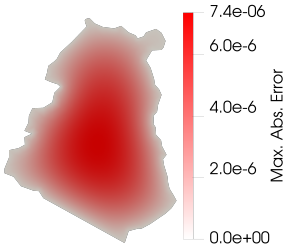

(d) Recovered individuals.

Figure 8: Maximum absolute error for each state variable.

In order to make the solution obtained even closer to the exact solution, the second mesh was refined again with the help of Gmsh *software*. The third discretization in the Figure 9 had 1660 nodes and 3159 finite elements.

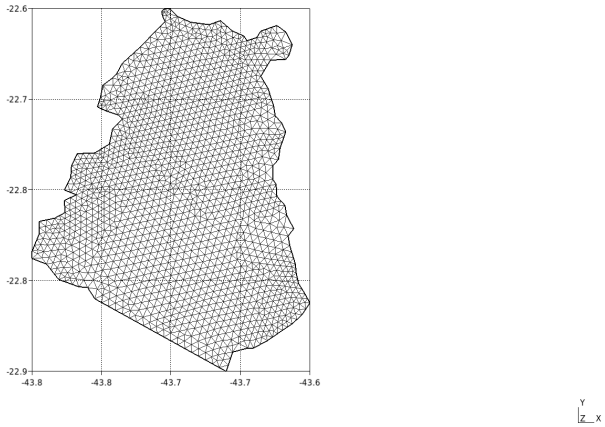

Figure 9: Third discretization of the spatial domain Ω of the model.

The maximum absolute errors for each state variable of the third discretization are illustrated below:

- Error graph for the third discretization of the spatial domain Ω:

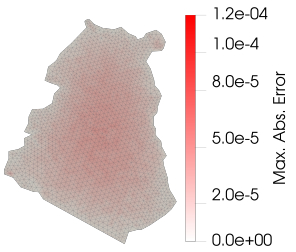

(a) Dengue vectors.

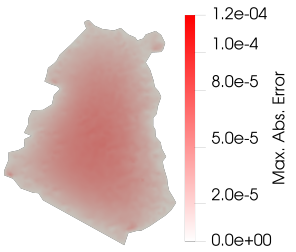

(b) Susceptible individuals.

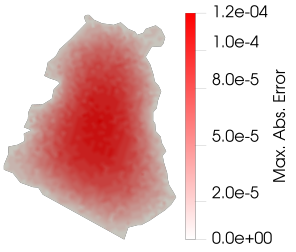

(c) Infected individuals.

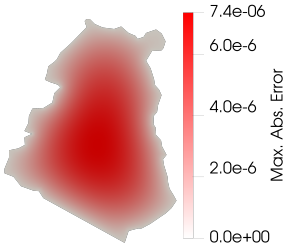

(d) Recovered individuals.

Figure 10: Maximum absolute error for each state variable .

Based on the graphs generated by ParaView, we recorded the maximum absolute errors that each state variable M, S, I, R obtained for each mesh in the table 1.

Table 1: Maximum absolute error for the MSIR model variables at different mesh refinements.

	Nodes	Elements	**M**	**S**	**I**	**R**
Mesh 1	473	860	$6.9 \cdot 10^{-4}$	$2.0 \cdot 10^{-4}$	$2.0 \cdot 10^{-4}$	$0.07 \cdot 10^{-4}$
Mesh 2	893	1672	$1.2 \cdot 10^{-4}$	$1.2 \cdot 10^{-4}$	$1.2 \cdot 10^{-4}$	$0.07 \cdot 10^{-4}$
Mesh 3	1660	3159	$1.2 \cdot 10^{-4}$	$1.2 \cdot 10^{-4}$	$1.2 \cdot 10^{-4}$	$0.07 \cdot 10^{-4}$

This factor shows us that a finer mesh is the best option for a simulation, due to the improved accuracy of the approximate solution. The next step in the research will be to simulate the dengue epidemic during December 2023 to February 2024 for the mesh used in the example, taking into account factors such as rainfall indices, number of containers with accumulated water, and geographic data provided by the municipal government.

5 Conclusion

The main objective of this work was the development and validation of the computational implementation, based on the Finite Element Method (FEM), to solve the system of PDEs for the MSIR model of dengue spatial propagation. Validation was performed using a test problem with a known exact solution.

Since the maximum error of order 10^{-4} is within the expected range for the simulation, it's believed that the FEM implementation was successful. The convergence analysis showed that refining the spatial mesh representing the continuous domain of the Seropédica region, by increasing the number of nodal points, led to a reduction in the maximum absolute error across all state variables of the model M, S, I, R. This factor indicates that a more refined mesh is the best option for a simulation, due to the improved precision of the approximate solution.

The next step in the research will be to simulate the dengue epidemic from December 2023 to February 2024 for the mesh used in the example, taking into account factors such as rainfall indices, the quantity of water-accumulating receptacles, and geographical data provided by the municipality's city hall.

AUTHOR CONTRIBUTIONS. This work was developed as part of an ongoing undergraduate research project.

- Amanda Maria Cardoso Cabral: Writing; Conceptualization; Methodology; Results; Validation; Visualization.
- Edivaldo Figueiredo Fontes Junior: Supervision; Support for mathematical calculations; Support in model simulation; Review.

CONFLICT OF INTEREST. The authors declare no conflict of interest regarding the publication of this preprint. The research was supported by the Rio de Janeiro State Research Support Foundation (FAPERJ).

DATA AVAILABILITY. The conclusions of this research are based on the results obtained from the simulations. The parameters, equations, and results that support the analyses are contained in the text.

FUNDING. The research is being supported by the Rio de Janeiro State Research Support Foundation (FAPERJ).

References

Ahrens, J., Geveci, B., and Law, C. (2005). ParaView: An end-user tool for large data visualization. In *Visualization Handbook*. Elsevier.

Almeida, P. R. d. (2014). Modelos epidêmicos sir, contínuos e discretos, e estratégias de vacinação. Master's thesis, Universidade Federal de Viçosa.

Atkins, P. and de Paula, J. (2018). *Princípios de Química: Questionando a Vida Moderna e o Meio Ambiente*. Bookman, Porto Alegre, 7 edition.

Barelli, V. E. G., Bigardi, T. M., and Minatogau, F. S. (2023). Aplicação do modelo sir com dinâmica vital no estudo da transmissão da dengue no município de campinas - sp. *Biomatemática*, 33:115–130. Publicação da Ilum Escola de Ciência, C. N. Pesquisa em Energia e Materiais.

Burden, R. L. and Faires, J. D. (2011). *Numerical Analysis*. Cengage Learning, Boston, 9 edition. Seção 2.2: The Newton-Raphson Method. Método de Newton aplicado à resolução numérica de equações.

Crank, J. and Nicolson, P. (1947). A practical method for numerical evaluation of solutions of partial differential equations of the heat-conduction type. *Proceedings of the Cambridge Philosophical Society*, 43(1):50–67.

do Carmo, E. G. D., Fontes, E. F., Mansur, W. J., and Santos, M. F. F. (2024). Analysis of steady-state nonlinear problems via gradual introduction of nonlinearity. *Communications in Nonlinear Science and Numerical Simulation*, 128:107644.

Geuzaine, C. and Remacle, J.-F. (2009). Gmsh: A 3-d finite element mesh generator with built-in pre- and post-processing facilities. *International Journal for Numerical Methods in Engineering*, 79(11):1309–1331.

Gomes, L. T. (2009). Um estudo sobre o espalhamento da dengue usando equações diferenciais parciais e lógica fuzzy. Master's thesis, Universidade Estadual de Campinas (UNICAMP).

Gurgel-Gonçalves, R., Oliveira, W. K. d., and Croda, J. (2024). A maior epidemia de dengue no brasil: Vigilância, prevenção e controle. *Revista da Sociedade Brasileira de Medicina Tropical*, 57:e00203–2024. Publicado em 20 de setembro de 2024.

Hamer, W. H. (1906). Epidemic disease in england. *The Lancet*, 1:733–739.

Hughes, T. J. R. and Hughes, T. (2000). *The Finite Element Method: Linear Static and Dynamic Finite Element Analysis*. Dover Publications.

Instituto Brasileiro de Geografia e Estatística (IBGE) (2024). Cidades e Estados: Seropédica, RJ. https://www.ibge.gov.br/cidades-e-estados/rj/seropedica.html. Acessado em: 22 de julho de 2025.

Kermack, W. O. and McKendrick, A. G. (1927). A contribution to the mathematical theory of epidemics. *Proceedings of the Royal Society of London. Series A, Containing Papers of a Mathematical and Physical Character*, 115(772):700–721.

MBI Brasil (2024). Seropédica, RJ. https://www.mbi.com.br/mbi/biblioteca/cidade/seropedica-rj-br/. Acessado em: 22 de julho de 2025.

Mendonça, F. d. A., Souza, A. V. e., and Dutra, D. d. A. (2009). Saúde pública, urbanização e dengue no brasil. *Sociedade e Natureza*, 21(3):391–404.

Ministério da Saúde (2024). Dengue - situação epidemiológica. https://www.gov.br/saude/pt-br/assuntos/noticias/dengue. Acessado em: 08 abr. 2025.

Prefeitura Municipal de Seropédica (2023). *Site Oficial*. Prefeitura Municipal de Seropédica. Disponível em: https://seropedica.rj.gov.br/. Acessado em: 22 de julho de 2025.

Santos, M. F. F., do Carmo, E. G. D., Fontes, E. F., and Mansur, W. J. (2022). A scheme for the analysis of primal stationary boundary value problems based on fe/fd multi-method. *Finite Elements in Analysis and Design*, 209:103809.

This preprint was submitted under the following conditions:

- The authors declare that they are aware that they are solely responsible for the content of the preprint and that the deposit in SciELO Preprints does not mean any commitment on the part of SciELO, except its preservation and dissemination.
- The authors declare that the necessary Terms of Free and Informed Consent of participants or patients in the research were obtained and are described in the manuscript, when applicable.
- The authors declare that the preparation of the manuscript followed the ethical norms of scientific communication.
- The authors declare that the data, applications, and other content underlying the manuscript are referenced.
- The deposited manuscript is in PDF format.
- The authors declare that the research that originated the manuscript followed good ethical practices and that the necessary approvals from research ethics committees, when applicable, are described in the manuscript.
- The authors declare that once a manuscript is posted on the SciELO Preprints server, it can only be taken down on request to the SciELO Preprints server Editorial Secretariat, who will post a retraction notice in its place.
- The authors agree that the approved manuscript will be made available under a Creative Commons CC-BY license.
- The submitting author declares that the contributions of all authors and conflict of interest statement are included explicitly and in specific sections of the manuscript.
- The authors declare that the manuscript was not deposited and/or previously made available on another preprint server or published by a journal.
- If the manuscript is being reviewed or being prepared for publishing but not yet published by a journal, the authors declare that they have received authorization from the journal to make this deposit.
- The submitting author declares that all authors of the manuscript agree with the submission to SciELO Preprints.